Tomographic Reconstruction of Sound Velocity Distribution in the Breast Using Linear Arrays

Sheng-Wen Huang[1,2] and Pai-Chi Li[1,2]
[1]Department of Electrical Engineering, National Taiwan University
[2]Division of Medical Engineering Research, National Health Research Institutes
Taipei, Taiwan, R. O. C.

Abstract - An approach based on limited-angle transmission tomography for reconstruction of the sound velocity distribution in the breast is proposed. The imaging setup allows acoustic data acquisition for simultaneous B-mode image formation and the tomographic sound velocity reconstruction. The time-of-flight data are acquired by a linear array positioned at the top of the compressed breast that both transmits and receives, and a metal plate is placed at the bottom as a reflector. In order to improve the sound velocity estimation accuracy, a reconstruction algorithm based on a convex programming formulation has been developed. Simulations for both imaging and time-of-flight data based on a 5-MHz linear array were performed. Effects of wave propagation such as refraction and diffraction were included in the generated data. Results show that the proposed approach is both feasible and accurate. The approach can be used to complement conventional B-mode imaging to enhance the detection of breast cancer.

I. INTRODUCTION

The detection of breast cancer is an important task of medical ultrasound. In B-mode imaging, the image contrast is primarily determined by tissue scattering properties and acoustic impedance. Therefore, two regions with similar scattering properties and acoustic impedance are hardly distinguishable. For example, the B-mode image of a solid homogeneous hypoechoic tumor with irregular borders may look like a fat region [1]. In order to provide a higher contrast among different tissues of interest, alternative imaging methods can be used to form breast images based on different acoustic parameters.

In this paper, the physical parameter of interest is the sound velocity because the velocity of sound in cancerous tissue is higher than that in fat [2]. The main purpose of this paper is to develop an imaging strategy for reconstructing the sound velocity distribution using pulse-echo data from a linear array, such as that used in B-mode imaging. Note that the setup is similar to the limited-angle transmission tomography setup proposed by Krueger *et al.* [3]. Nonetheless, a reconstruction algorithm is proposed that provides a significant improvement in estimation accuracy. This improvement is mainly attributable to the proposed technique successfully incorporating information from the B-mode image of the same object. As described in Section III and IV, the B-mode image is utilized for segmentation such that constraints can be properly defined and imposed during reconstruction. Simulations were performed to test the efficacy of the proposed technique.

II. IMAGING SETUP

The imaging setup is shown in Fig. 1. The image objects used in this paper contain cylindrical targets along the z-axis, and t denotes the time. Note that the setup is similar to the one proposed by Krueger *et al.* [3][4]. Figure 1 shows that the linear array has several (N_A) channels and that a metal plate is used for reflecting the acoustic wave. The array axis and the beam axis are defined as the x-axis and the y-axis, respectively. In addition to performing B-mode imaging, the imaging setup shown in Fig. 1 is also capable of transmitting a wideband pulse $g(t)$ from a single channel in order to acquire a complete channel data set $\{e_{ij}(t)\}, 1 \le i, j \le N_A$, where $e_{ij}(t)$ is the echo signal received by channel j when only channel i transmits. With $e_{ij}(t)$, the time-of-flight t_{ij} corresponding to the same transmit/receive combination for the echo reflected from the bottom metal plate can be obtained.

Let $c(x, y)$ denote the sound velocity at the center frequency of the transmitted pulse. Under the assumption of the straight-line propagation path,

$$t_{ij} = \int_{L_{ij}} s(x,y)dl\,, \tag{1}$$

where L_{ij} is the path of the line integral as shown in Fig. 1, and $s(x,y) = c^{-1}(x,y)$ is defined as the slowness. Assume the background slowness in the image object is s_0, and define

$$t_{ij,0} = \int_{L_{ij}} s_0 dl \tag{2}$$

as the geometrical delay, then the time-of-flight with geometrical delay compensated becomes

$$\Delta t_{ij} = t_{ij} - t_{ij,0} = \int_{L_{ij}} [s(x,y) - s_0]dl = \int_{L_{ij}} \Delta s(x,y)dl\,. \tag{3}$$

$\Delta s(x,y)$ can be discretized with spatial sampling intervals Δx_{s} and Δy_{s} in the x and y directions, respectively. In this case, (3) becomes

$$\Delta t_{ij} = \sum_{n=1}^{N}\sum_{m=1}^{M} \Delta s(m,n) l_{ij}(m,n) = \mathbf{l}_{ij}^{\mathrm{T}} \Delta\mathbf{s}\,, \tag{4}$$

where $\mathbf{l}_{ij}$ and $\Delta\mathbf{s}$ are $MN\times 1$ column vectors, $(\mathbf{l}_{ij})_{(m-1)N+n} \equiv l_{ij}(m,n)$ is the contribution of grid point (m,n), $1 \le m \le M$, $1 \le n \le N$, and $(\Delta\mathbf{s})_{(m-1)N+n} \equiv \Delta s(m,n)$.

There are a total of N_{A}^2 equations in (4). Due to the assumption of the straight-line propagation path, $\mathbf{l}_{ij} = \mathbf{l}_{ji}$, and Δt_{ij} can be set to $(\Delta t_{ij} + \Delta t_{ji})/2$ for $1 \le i \le N_{\mathrm{A}}$, $1 \le j \le i$. Thus, the number of equations reduces to $N_{\mathrm{A}}(N_{\mathrm{A}}+1)/2$ and they can be put into the following matrix form:

$$\mathbf{L}\Delta\mathbf{s} = \Delta\mathbf{t}\,, \tag{5}$$

where $\Delta\mathbf{t} = \left[\Delta t_1 \;\; \Delta t_2 \;\; \cdots \;\; \Delta t_{N_{\mathrm{A}}(N_{\mathrm{A}}+1)/2}\right]^{\mathrm{T}}$ and $\mathbf{L} = \left[\mathbf{l}_1 \;\; \mathbf{l}_2 \;\; \cdots \;\; \mathbf{l}_{N_{\mathrm{A}}(N_{\mathrm{A}}+1)/2}\right]^{\mathrm{T}}$. In (5), $\Delta\mathbf{t}$ is obtained from the channel data, and $\mathbf{L}$ is calculated based on the geometry.

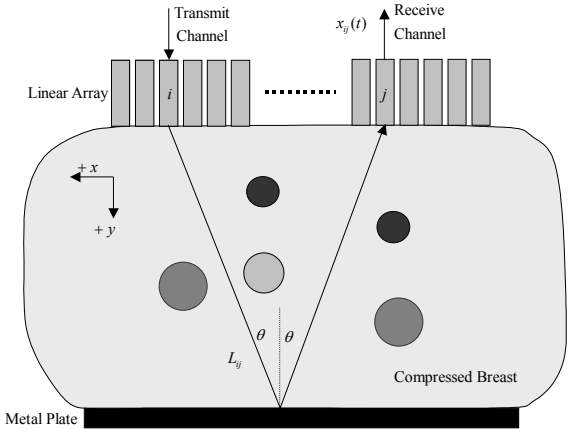

Fig. 1. Imaging setup analyzed in this paper.

III. RECONSTRUCTION OF THE SOUND VELOCITY DISTRIBUTION

A convex programming formulation for inconsistent problems [5] was chosen to solve (5) because it can incorporate the B-mode image information.

In order to satisfy (5), the slowness distribution $\Delta\mathbf{s}$ must belong to

$$C_{\Delta t_i} = \left\{\mathbf{x} \in \mathbf{R}^{MN} : \langle \mathbf{x}, \mathbf{l}_i \rangle = \Delta t_i \right\} \tag{6}$$

for $i = 1,2,\cdots, N_{\mathrm{A}}(N_{\mathrm{A}}+1)/2$. That is, $\Delta\mathbf{s}$ must belong to $\bigcap C_{\Delta t_i}$. $\bigcap C_{\Delta t_i}$ may be empty, and even if it is nonempty, the points in the set may not lead to reasonable sound velocities. Therefore, each $C_{\Delta t_i}$ is a soft-constraint set. The slowness distribution $\Delta\mathbf{s}$ does not have to match all time-of-flight data. Nonetheless, the distribution must minimize the total amount of violation of the time-of-flight data

$$\Phi^{\mathrm{s}}(\mathbf{x}) = \frac{1}{2}\sum_{i=1}^{N_{\mathrm{A}}(N_{\mathrm{A}}+1)/2} w_i d^2(\mathbf{x}, C_{\Delta t_i})\,, \tag{7}$$

where $w_i \in (0,1]$ for all i, $\sum w_i = 1$, and $d(\mathbf{x}, C_{\Delta t_i})$ is the distance between $\mathbf{x}$ and $C_{\Delta t_i}$.

To achieve good reconstruction accuracy, prior knowledge of $\Delta\mathbf{s}$ must be utilized. The sound velocity is assumed to be in $[c_{\mathrm{lower}}, c_{\mathrm{upper}}]$ (where $c_{\mathrm{lower}} = 1450$ m/s and $c_{\mathrm{upper}} = 1580$ m/s in the paper) and a hard-constraint set (i.e., $\Delta\mathbf{s}$ must belong to this set) is defined as follows,

$$C_{\mathrm{velocity}} = \left\{\mathbf{x} \in \mathbf{R}^{MN} : x_l \in [c_{\mathrm{upper}}^{-1} - s_0, c_{\mathrm{lower}}^{-1} - s_0], \; 1 \le l \le MN\right\}. \tag{8}$$

Using C_{velocity} as the unique hard-constraint set is not sufficient to obtain an accurate sound velocity distribution. Consider a B-mode image in which an object contains a region of interest surrounded by the background. Suppose that this region can be identified and segmented, then the following hard-constraint set can be generated:

$$C_{\mathrm{image}} = \left\{\mathbf{x} \in \mathbf{R}^{MN} : x_{b_1} = x_{b_2} = \cdots = x_{b_{N_{\mathrm{b}}}}, x_{r_1} = x_{r_2} = \cdots = x_{r_{N_{\mathrm{r}}}}, x_{br_i} \in F, 1 \le i \le N_{\mathrm{br}}\right\}, \tag{9}$$

where $I_{\mathrm{b}} \equiv \{b_1, b_2, \cdots, b_{N_{\mathrm{b}}}\}$ is the background index set, $I_{\mathrm{r}} \equiv \{r_1, r_2, \cdots, r_{N_{\mathrm{r}}}\}$ is the region-of-interest index set, $I_{\mathrm{br}} \equiv \{br_1, br_2, \cdots, br_{N_{\mathrm{br}}}\}$ is the boundary index set, and F is the closed interval with x_{b_1} and x_{r_1} as its end points. (9) means that all the slowness values in the background must be the same, and all the slowness values in the region of interest must also be the same. In addition, each slowness value at the boundary must be between that of the background and that of the region of

interest. Note that no specific slowness value has been set in any region at this point. C_{image} can be similarly generated when the object contains more regions of interest.

A reconstruction algorithm was developed to find a slowness distribution $\mathbf{x} \in C_{\text{velocity}} \bigcap C_{\text{image}}$ minimizing (7). In this algorithm, such an $\mathbf{x}$ is found by taking $\mathbf{x} = \lim_{n\to\infty} \mathbf{x}_n$. $\mathbf{x}_0 \in C_{\text{velocity}} \bigcap C_{\text{image}}$ is an initial slowness distribution, and

$$\mathbf{x}_{n+1} = \frac{1}{2}\left\{\mathbf{x}_n + P_{C_{\text{velocity}}\cap C_{\text{image}}}\left[\sum_{i=1}^{N_A(N_A+1)/2} w_i P_{C_{\Delta t_i}}(\mathbf{x}_n)\right]\right\}, n \geq 1, \quad (10)$$

where $P_{C_{\text{velocity}}\cap C_{\text{image}}}$ is the projector onto $C_{\text{velocity}} \bigcap C_{\text{image}}$. In this paper, all weights w_i were set to be the same (i.e., each time-of-flight is equally important).

IV. NUMERICAL RESULTS

In all cases shown below an array with $N_A = 234$ and a pitch of 0.15 mm (giving an array width of 35.1 mm) was used. The distance between the array and the metal plate was 35 mm. Each array channel has a Gaussian frequency response with a center frequency of 5 MHz and a two-way –12 dB fractional bandwidth of 0.6. All array elements are assumed to be a line source. The other parameters were $\Delta x_s = 0.5$ mm, and $\Delta y_s = 0.5$ mm.

The time-of-flight data were generated using the series solution to the scattering of a plane wave incident on a fluid cylinder [6]. Figure 2 outlines the procedure.

The B-mode images were simulated using a *k*-space method [7]. To reduce the computation time, only eight channels (channels 27, 53, 79, 105, 130, 156, 182, and 208) were used on transmit in turn, and only receive channels with j values obeying $|j-i| \leq 26$ were used on receive when channel i was fired. Figure 3 outlines the procedure for extracting the segment information .

An object comprising a background of glandular material with a cylinder of fat with a radius of 4 mm at its center was considered first as an example. The corresponding parameters of the different materials are listed in Table I. The corresponding B-mode image is shown in Fig. 4(a). After applying a threshold to the processed B-mode image, the fat region was extracted as shown in Fig. 4(b). The boundary between the fat region and the background was directly derived from the segmented fat region by morphological dilation [9] as shown in Fig. 4(c).

TABLE I
PHYSICAL PARAMETERS

Material	Sound velocity (m/s)	Density (g/cm^3)	Absorption (dB/cm/MHz)
Glandular	1521	1.05	1.136
Fat	1471	0.94	0.536
Tumor	1549	1.12	1.478

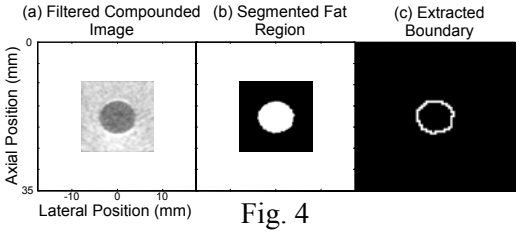

Fig. 4

Figure 5(a) and (b), 5(c) and (d), and 5(e) and (f) show the estimation results corresponding to cylinders with radii of 4 mm, 2 mm, and 6 mm, respectively. Define errors as

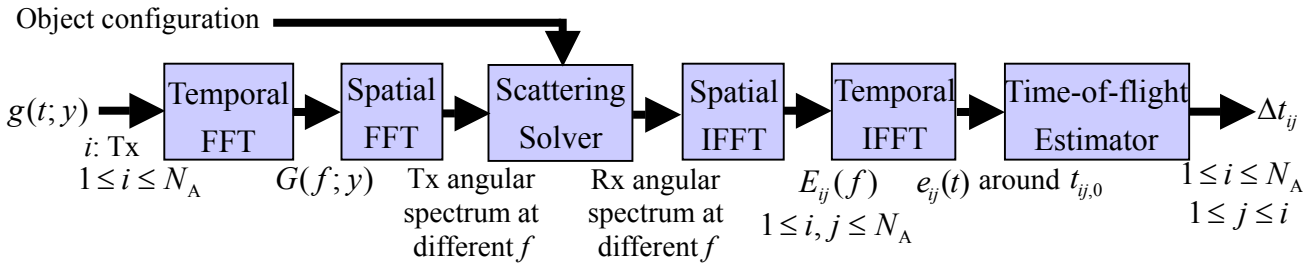

Fig. 2 Generation of time-of-flight data.

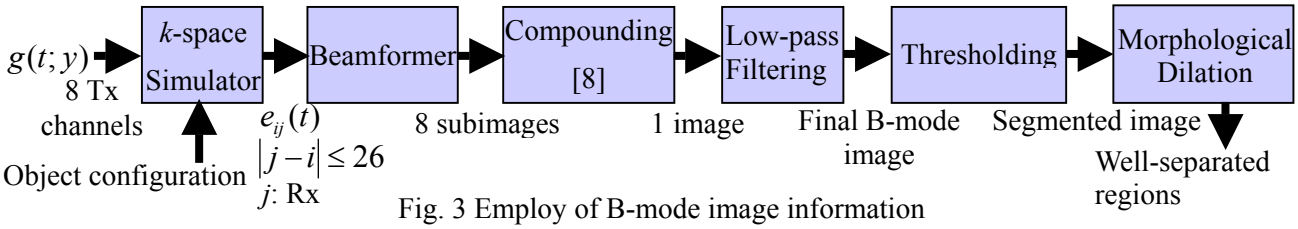

Fig. 3 Employ of B-mode image information

$$\Delta c_{(\cdot)} = c_{(\cdot),\text{reconstructed}} - c_{(\cdot),\text{true}}, \qquad (11)$$

where $(\cdot)$ denotes b (background) or c (cylinder). The upper panels (5(a), (c), and (e)) are the sound velocity distributions and the lower panels (5(b), (d), and (f)) are the sound velocity errors. The Δc_c values are –2.6 m/s, –0.1 m/s, and –1.4 m/s, respectively, and those of Δc_b are 0.0 m/s, 0.1 m/s, and 0.0 m/s, respectively.

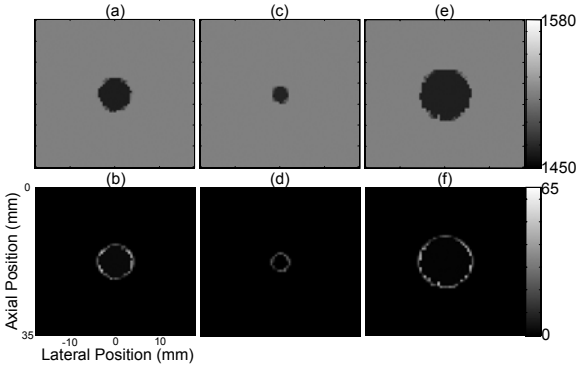

Fig. 5 (a),(c),(e) Reconstructed sound velocity distributions. (b),(d),(f) Reconstruction errors.

An object comprising a background of glandular material with three cylinders, all with a radius of 4 mm, was also used to test the proposed algorithm. The geometry of the object is shown in Fig. 6(a). The first cylinder was assigned the physical parameters of fat except for the sound velocity, which was set to 1496 m/s. The second cylinder was assigned the parameters of a tumor, and the third cylinder was assigned those of fat. The B-mode image is shown in Fig. 6(b). Figure 6(c) shows the segmentation result. These small regions in the background were automatically removed during boundary extraction due to their smaller size; the boundaries are shown in Fig. 6(d). The reconstructed sound velocity distribution is shown in Fig. 6(e) and the sound velocity error is shown in Fig. 6(f). In this case, $\Delta c_b = 0.3$ m/s , $\Delta c_{c,1} = -3.2$ m/s , $\Delta c_{c,2} = 1.2$ m/s , and $\Delta c_{c,3} = 0.4$ m/s .

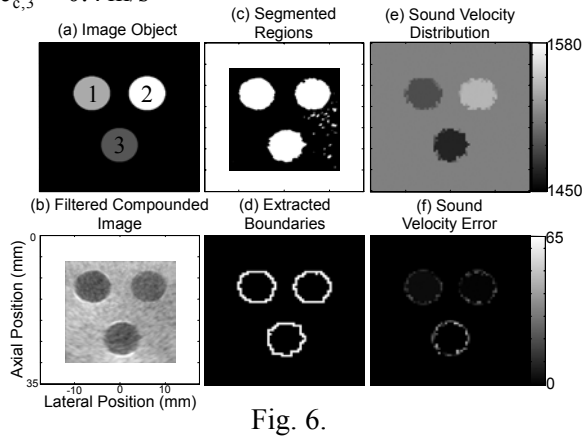

Fig. 6.

V. CONCLUSIONS

Here we have proposed a method for incorporating the segmentation information of a B-mode image into the process of sound velocity reconstruction with limited-angle transmission tomography. A *k*-space method was utilized to simulate the B-mode images, and the series solution to the scattering of a plane wave incident on a fluid cylinder was utilized to generate the required time-of-flight data. Effects of wave propagation such as refraction and diffraction were included in the generated data. In the cases considered in this paper, the reconstructed sound velocities are accurate except at the boundaries. Simulation results based on a 5-MHz linear array show that the sound velocity error was generally 1–3 m/s. The radius of the object under investigation was 2–6 mm, and all the objects were detected successfully. With this method, obtaining the sound velocity distribution is feasible with current B-mode imaging setup using linear arrays.

REFERENCES

[1] M. E. Lanfranchi, *Breast Ultrasound*, 2nd ed., NY: Marban Books, 2000.

[2] S. A. Goss, R. L. Johnston and F. Dunn, "Comprehensive compilation of empirical ultrasonic properties of mammalian tissues," *J. Acoust. Soc. Am.*, vol. 64, no. 2, pp. 423–457, 1978.

[3] M. Krueger, A. Pesavento and H. Ermert, "A modified time-of-flight tomography concept for ultrasonic breast imaging," in *Proc. IEEE Ultrason. Symp.*, 1996, pp. 1381–1385.

[4] M. Krueger, V. Burow, K. M. Hiltawsky and H. Ermert, "Limited angle ultrasonic transmission tomography of the compressed female breast," in *Proc. IEEE Ultrason. Symp.*, 1998, pp. 1345–1348.

[5] P. L. Combettes and Pascal Bondon, "Hard-constrained inconsistent signal feasibility problems," *IEEE Trans. Signal Processing*, vol. 47, no. 9, pp. 2460–2468, 1999.

[6] P. M. Morse and K. U. Ingard, *Theoretical Acoustics*, NY: McGraw-Hill, 1968.

[7] M. Tabei, T. D. Mast and R. C. Waag, "A *k*-space method for coupled first-order acoustic propagation equations," *J. Acoust. Soc. Am.*, vol. 111, no. 1, pp. 53–63, 2002.

[8] M. O'Donnell and S. D. Silverstein, "Optimal displacement for compound image generation in medical ultrasound," *IEEE Trans. Ultrason. Ferroelectr. Freq. Control*, vol. 35, no. 4, pp. 470–476, 1988.

[9] R. C. Gonzalez and R. E. Woods, *Digital Image Processing*, 2nd ed., Mass.: Addison-Wesley, 2002.